

MITIGATION OF VIBRATIONS INDUCED BY RAILWAY TRAFFIC THROUGH SOIL BURIED INCLUSIONS: A NUMERICAL STUDY

PACS NO. 43.40

Alexandre Castanheira Pinto¹; Pedro Alves Costa¹; Luís Godinho²; Paulo Amado Mendes²

¹Construct-FEUP, University of Porto, Rua Dr. Roberto Frias, 4200-465 Porto, Portugal

amgcpinto@fe.up.pt ; pacosta@fe.up.pt

²ISISE, Dep. Civil Engineering, University of Coimbra, Pólo II, Rua Luís Reis Santos, 3030-788 Coimbra, Portugal

lgodinho@dec.uc.pt; pamendes@dec.uc.pt

KEYWORDS: Railway engineering; Mitigation measure; 2.5D FEM-PML; Numerical study; Soil buried inclusion.

ABSTRACT

The topic of vibration induced by rail traffic has received a special attention from the scientific community over the last decades. Thus, procedures to minimize the discomfort caused by an efficient railway network have to be proposed. In this paper a preliminary numerical study is presented about the mitigation of vibrations based in the introduction in the ground of a set of inclusions parallel to the railway track. Analysis in space-frequency, and frequency-wavenumber domain allowed concluding that the ground wave-propagation is strongly affected by the inclusions presence. Indeed, theoretical simple equations were derived and here proposed in order to allow the engineering tuning of the solution.

1 INTRODUCTION

Vibrations induced by human activities, such as construction or traffic, have become a relevant concern of modern societies. Despite these kind of vibrations usually does not reach a level that can put in risk the structural safety of nearby facilities, the long term continuous exposition of population to vibrations is nowadays recognized as a public health problem [1, 2]. In this scope, transportation infrastructures in urbanized regions should receive special attention, namely in the case of railways, since the demand for increasing the railway infrastructure capacity in European countries is defined in the roadmap for railway 2050. The increase of railway infrastructure capacity will demand efficient solutions for vibration mitigation in order to achieve the societal acceptance of this goal. Actually, the topic of mitigation of vibrations induced by railway traffic has received a considerable attention by the technical and scientific communities, where different solutions have been proposed and analyzed. Usually, the distinct solutions are grouped in function of their location: i) at the source, as for instance introduction of resilient elements at track level, [3, 4]; ii) at the receiver, through the change of the dynamic of the receiver (building), [5, 6]. Alternatively to these two solutions, mitigation measures can be applied at the propagation path, trying by that way to minimize, or at least to change, the energy that impinges the facilities to protect.

Despite of the recent advances in the topic, the exploration of the potential given by phononic acoustic materials, a specific class that can be framed within the so-called metamaterials, has not been extensively analyzed in this context yet. Actually, the propagation of almost all types of waves such as ultrasound, acoustic, elastic, and even electromagnetic and thermal in specific classes of periodic structures known as phononic or acoustic metamaterials, has drawn the interest of a large number of scientists and engineers [7]. The present paper aims to give a contribution for the development of vibration shielding solutions based in the introduction of periodic arrays of inclusions parallel to railway infrastructures. The paper starts with a deep analysis of the phenomena following a step-by-step approach, where the physical phenomena are analyzed in the space-frequency and in the wavenumber-frequency domains.

2 BRIEF DESCRIPTION OF THE NUMERICAL APPROACH

Transportation infrastructures, such as roads, railways tracks, pipes, can be often assumed as infinite and longitudinally invariant structures. In such conditions, if the assumption of linear response can be faced as reasonable, it is possible to achieve the 3D wave propagation solution by a 2.5D approach, where the equilibrium equations are formulated in the wavenumber-frequency domain. This approach takes hand of the Fourier transformation regarding the longitudinal development direction and, by that reason, only the cross-section needs to be discretized.

In the space-frequency domain, the fundamental wave propagation equation is given by:

$$(\lambda + 2\mu)\nabla\nabla * u - \mu\nabla * \nabla * u + \omega^2\rho * u = 0 \quad (1)$$

where $u(x, y, z, \omega)$ is the displacement vector, λ and μ are the Lamé's constants and ρ is the mass density of the elastic medium. Considering now the situation depicted in Figure 1, the 3D solution can be obtained through the combination of several space-harmonic solution through the application of a Fourier transform regarding the longitudinal direction.

In the present study a 2.5D finite element approach is followed, since it allows dealing easily with complex geometries. A PML technique is applied to avoid the spurious wave reflection in the artificial boundaries [8]. Following the 2.5D FEM-PML approach and after the assemblage of the equations of each individual element, the equilibrium condition is established by the following equation:

$$\{[K_{FEM}^g(k_1)] + [K_{PML}^g(k_1, \omega)] - \omega^2([M_{FEM}^g] + [M_{FEM}^g(k_1, \omega)])\}u_n(k_1, \omega) = p_n(k_1, \omega) \quad (2)$$

Where k_1 is the wavenumber, ω is the frequency, u_n is the vector of nodal displacements in the transformed domain, p_n is the vector of external nodal loads in the transformed domain. The matrices $[K_{FEM}^g]$ and $[K_{PML}^g]$ are the global stiffness matrices of the FEM domain and of the PML domain, respectively, while $[M_{FEM}^g]$ and $[M_{PML}^g]$ are the corresponding global mass matrices.

The solution on the space-frequency domain or in the space-time domain is finally obtained through inverse Fourier operations. Details about procedure can be found in following references: [10, 11]

3 DYNAMIC RESPONSE OF THE SYSTEM WITH A SINGLE INCLUSION

Buried inclusions in the ground change the wave propagation pattern and can be used as mitigation countermeasures. If these inclusions are installed with a certain array, constituting a periodic structure, a phononic metastructure can be achieved and shielding effect is expected to be reached in certain frequency bands. The dynamic response of the system with the presence of a single stiff inclusion was already addressed by Coulier et al. [12]. For this example, it is considered a homogeneous half-space with a circular shape inclusion ($D=0.6\text{ m}$) buried at 0.4 m depth and with infinite development along the longitudinal direction as depicted in Figure 1. Superimposed in Figure 1 is a detail of the finite element mesh created to model the case study. Mechanical properties of the ground and inclusion are given in Table 1.

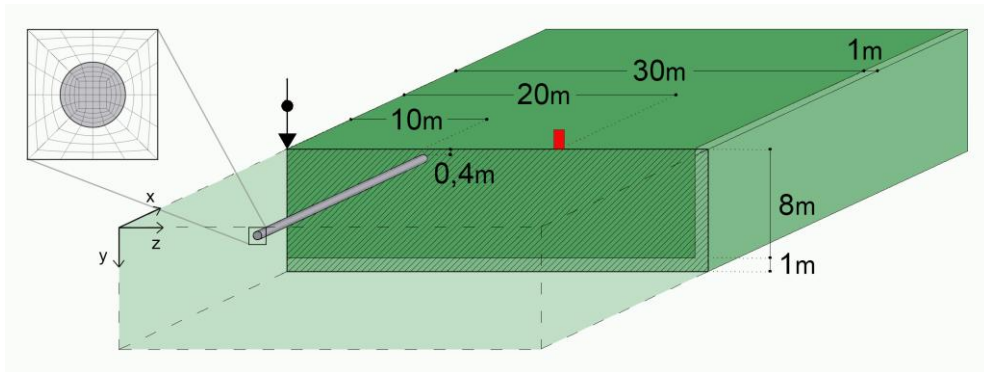
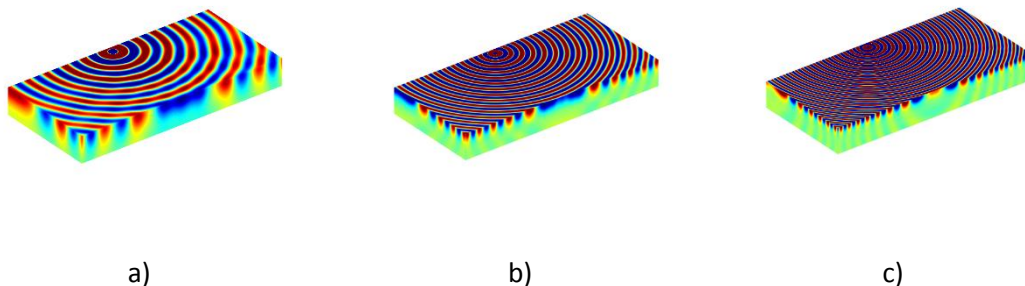


Figure 2 – Illustrative scheme of the geometry of the cross section.

Table 1 – Properties adopted for the different materials

Material	Density [Kg/m^3]	Young Modulus [MPa]	ν [-]	ζ [-]
Soil	1700	116	0.33	0.001
Inclusion	2700	4416	0.2	0.001

Figure 3 shows the real part of the vertical displacement field generated by a harmonic point load located at ground surface and 10 m away from the inclusion. Results are presented for several frequencies, being shown in the upper row the reference scenario (without inclusion) and in the lower row the vertical displacement field generated in similar conditions but in the presence of the inclusion. From Figure 3 it is obvious that perturbation induced by inclusion presence is highly dependent on the excitation frequency. Actually, for the frequency of 25 Hz, the displacement field is almost not affected by the inclusion presence. The previous fact is also evident in Figure 3a, where the insertion loss of the vertical (IL_{uz}), defined by equation 3, is plotted.



a)

b)

c)

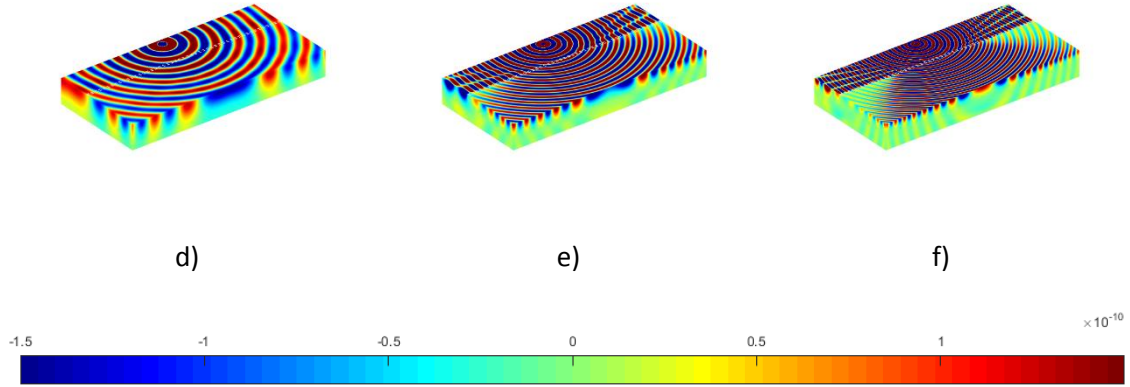


Figure 3 – Vertical displacement for homogeneous media: a) 25Hz; b) 50Hz; c) 75Hz; Vertical displacement for a medium with one inclusion: d) 25Hz; e) 50Hz; f) 75Hz.

$$IL_{uz} = 20 \log_{10} \left(\frac{|u_z^{ref}(x,y,z,\omega)|}{|u_z(x,y,z,\omega)|} \right) \quad (3)$$

However, from Figure 4b and Figure 4c it is possible to observe that with the increase of the frequency an attenuation effect is observed by the inclusion presence, being more evident for the excitation frequency of 75 Hz. Furthermore, the insertion loss contours depicted in Figure 4 show the formation of a cone, inside which the attenuation effect is almost negligible, but it is relevant in the outside region. This effect was previously explained by Coulier et al. [12] and it is due to the waveguided effect provided by the stiffer inclusion when the wavelength of waves propagating in the longitudinal direction along the ground is shorter than the wavelength of bending wave propagation along the inclusion in free condition.

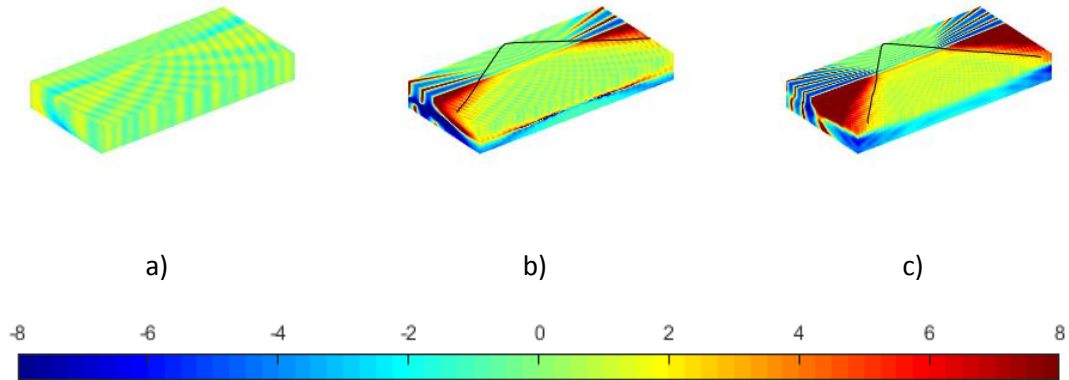


Figure 4 – Insertion loss [dB] of vertical displacement for single inclusion scenario and for frequencies of: a) 25Hz; b) 50Hz; c) 75Hz.

To better discern this effect, Figure 5 presents the insertion loss in the wavenumber-frequency domain for the alignment located 20 m away from the load, i.e., at 10 m distance of the inclusion. The wavenumber is normalized by the shear wavenumber:

$$K_1[-] = k_1 * \frac{C_s}{\omega} \quad (4)$$

where C_s is the shear wave velocity.

Only the propagation region is represented in the figure, since for wavenumber k_1 larger than the Rayleigh wavenumber only evanescent waves can propagate along the transversal direction. In the same figure, the free bending wave dispersion relationship of the inclusion is depicted by the black line. This dispersion relationship can be easily obtained assuming the inclusion as a Bernoulli-Euler beam:

$$K1 = \sqrt[4]{\frac{M * \omega^2 C_s}{EI \omega}} \quad (5)$$

where M is the mass of the inclusion and EI is the bending stiffness.

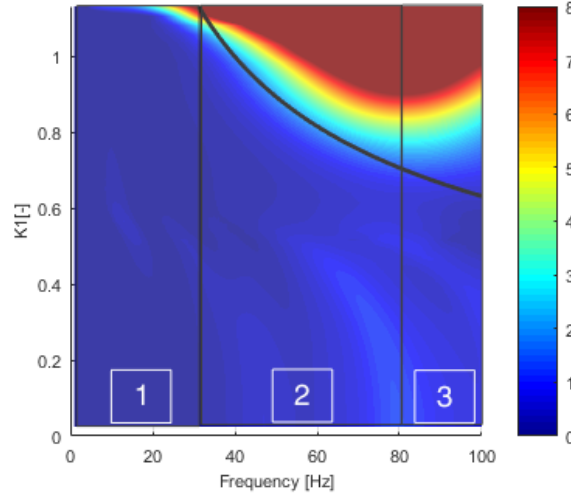


Figure 5 – Frequency-wavenumber of the insertion loss (dB) for the alignment 20m point away from the load (single inclusion).

As can be seen, attenuation effects can only be achieved for wavenumbers K_1 larger than those defined by the free-bending dispersion relationship of the inclusion. Actually, a detailed analysis of Figure 5 allows defining 3 zones of different behavior. The first zone corresponds to the frequency range up to the intersection between the dispersion relationships of the P-SV waves in the ground and of the free-bending of the beam. As shown by Coulier et al. [12], the limit of this frequency range is defined by equation 6, and for excitation frequencies lower than this limit there is no benefit induced by the inclusion presence.

$$\omega_c = C_R \sqrt{\frac{M}{EI}} \quad (6)$$

where C_R is the Rayleigh wave velocity.

However, passing the cut-on frequency defined by equation 6, positive insertion loss can be observed for values of k_1 larger than those defined by equation 5, which means that the presence of the inclusion avoids the propagation of vibrations along the transversal direction when the propagating wavelengths in the ground and in that direction are shorter than the free-bending wavelengths in the inclusion. In the space-frequency domain this effect is noticeable by the formation of the cone discussed above, with an opening angle defined by:

$$\theta = \sin^{-1} \left(\sqrt[4]{\frac{M * \omega^2}{EI} * \frac{C_R}{\omega}} \right) \quad (7)$$

The definition of the cone shadow region is easily achieved taking into account the decomposition of the propagating wavenumber k_R into the k_1 and k_2 , representing waves propagating into longitudinal and transversal directions respectively.

A third behavior zone is also detected in Figure 5, corresponding to frequencies larger than 80 Hz. In this range it is possible to see that positive values of IL are only visible for larger values of K_1 as the frequency increases. This effect, not noticed in the studies provided by Coulier et al. [12] neither by Barbosa et al. [13], is due to the fact that in the present study the inclusion is buried, not achieving the ground surface.

5 DYNAMIC RESPONSE FOR MULTIPLE INCLUSIONS: SINGLE ROW

As previously mentioned, the consideration of multiple inclusions allows taking benefit of the meta-structure behavior. This effect is added to the mitigation effect induced by the presence of a stiffer inclusion in a host medium, which behavior was already discussed in the previous section. Therefore, a new cross section is now considered, adopting two more inclusions parallel to the first one and in a center-to-center distance of 1.2m, as shown in Figure 6.

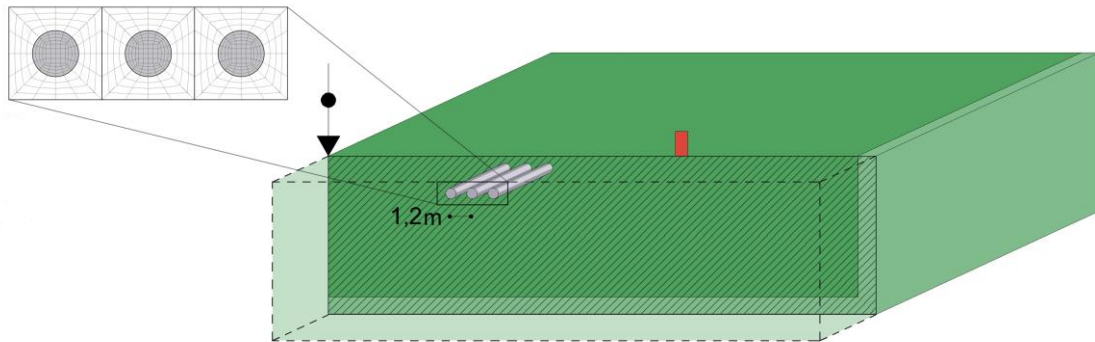


Figure 6 – Cross section with three parallel inclusion with a detail of the finite element mesh constructed.

Figure 7 shows the insertion loss of the vertical displacement on the frequency-space domain for frequencies of 25 Hz, 50 Hz and 75 Hz. Scrutinizing the results for the 25Hz and 50Hz, and comparing with homologous results depicted in Figure 4, it is observed that the behavior pattern persists: i) for the frequency of 25 Hz the inclusion presence almost doesn't affect the dynamic response of the system; ii) for the frequency of 50 Hz, there is a cone, inside which the mitigation of vibrations due to the presence of the inclusions is almost negligible. Despite the similarities of the dynamic response for single or for multiple inclusions when the excitation frequency is 50 Hz (Figure 7b), it should be mentioned that the presence of multiple inclusions allows to achieve higher values of IL, i.e., a more efficient mitigation is achieved when multiple inclusions are considered. A more interesting result is observed comparing Figure 4c and Figure 7c, i.e., the IL for the excitation frequency of 75Hz when single or multiple inclusions are considered, respectively. It is possible to see that in the first scenario (single inclusion) the area comprised inside the cone showed no attenuation on the vertical response (Figure 4c). On the other hand, for the case where multiple inclusions are considered, attenuation is also seen inside of the referred cone (Figure 7c). This fact must be related to some effect which is triggered only when more than one inclusion is adopted, proving the existence of a group behavior.

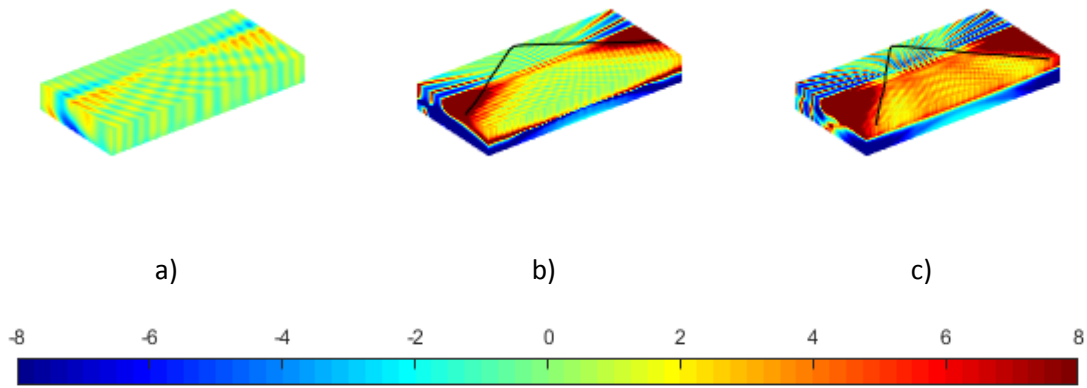


Figure 7 – Insertion loss [dB] of the vertical displacement for multiple inclusions scenario and for frequencies of: a) 25Hz; b) 50Hz; c) 75Hz.

To better discern the group effect previously identified, an analysis on the frequency-wavenumber domain is presented for a receiver located in the alignment 20m away from the load application point.

Figure 8 shows the IL for that alignment in the frequency-wavenumber domain, where it is possible to isolate four different regions. The first two correspond to the same ones already discussed for a single inclusion scenario (Figure 5), i.e., for frequencies lower than the cut-on frequency (see equation 6) no attenuation is observed, followed by the region where the wave-guided behavior is provided by the inclusions stiffness. In addition to the previously identified regions a new one appears, where a considerable IL is perceived even for plane-strain conditions, i.e. $k_1 = 0$. This expresses a new effect, resulting from a group interaction. This effect is responsible for the vibration attenuation in the region previously without attenuation, and can be called the “sonic-crystal” effect. The band gap induced by the sonic-crystal effect is delimited by the following equations:

$$f(\theta) = \frac{Cr}{2 * d * \cos \theta} \quad (8)$$

$$f(\theta) = \frac{Cr}{\sqrt{2} * d * \cos \theta} \quad (9)$$

where d represents the distance among two inclusions, and θ the incident wave angle.

Limits defined for the bandgap are also illustrated in Figure 8 by the brown lines.

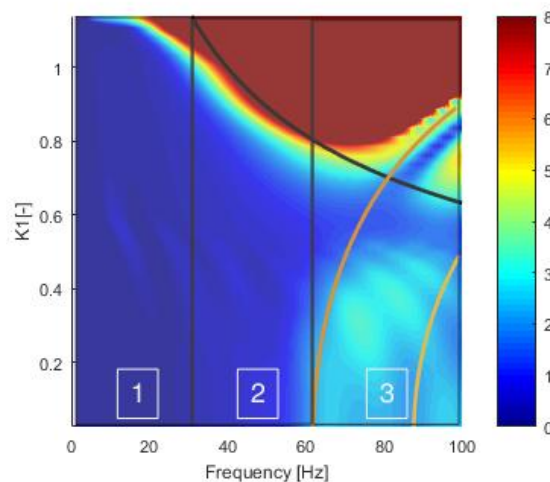


Figure 8 – Insertion loss in the frequency-wavenumber domain (dB) for the alignment 20m point away from the load (multiple inclusions scenario).

This band-gap effect is dependent on the distance between inclusions and on the wave propagation velocity of the host medium (assuming that the inclusions are much stiffer than the host medium).

6 CONCLUSIONS

In this paper, the authors presented a numerical study of a mitigation countermeasure which consists on a soil buried inclusions. For that task, a 2.5D FEM-PML approach was used to compute the 3D dynamic response. In this preliminary study, it was possible to identify the mechanical behavior pattern induced by the presence of a single inclusion. It was found that from a certain frequency value a wave-guided phenomenon is triggered, developing a cone which divides the space into two regions, one where is noticed an attenuation on the ground response and other where the vibration pattern is almost not altered. The open angle of the cone was found to be frequency dependent. For higher frequencies the wavelengths generated became very small in comparison with the buried depth of the inclusion and the energy starts to pass over it, inducing a loss of efficiency. An alternative scenario was considered where a row of three inclusions was adopted. This case showed an interesting efficiency improvement in comparison to the former scenario. Additionally to the previous attenuation mechanisms, a new one arises, caused by the interaction between the various inclusions, leading to positive insertion losses inside of the shadow cone. This group interaction is usually called the sonic crystal effect, and theoretical expressions are proposed to determine the frequency-wavenumber gap. The present study is still ongoing, where multiple scenarios taking advantage of the group interaction were constructed in order to evaluate the efficiency of the sonic crystal effect as a mitigation mechanism. It is also intended to evaluate the response for moving loads, simulating scenarios such as railway and road infrastructures.

ACKNOWLEDGEMENTS

This work was financially supported by: Project POCI-01-0145-FEDER-007457 -CONSTRUCT - Institute of R&D in Structures and Construction and Project POCI-01-0145-FEDER-007633 both funded by FEDER funds through COMPETE2020 - Programa Operacional Competitividade e Internacionalização (POCI) – and by national funds through FCT - Fundação para a Ciência e a Tecnologia; Project PTDC/ECMCOM/1364/2014. The authors are also sincerely grateful to European Commission for the financial sponsorship of H2020 MARIE SKŁODOWSKA-CURIE RISE Project, Grant No. 691135 “RISEN: Rail Infrastructure Systems Engineering Network”.

REFERENCES

1. Croy, I., M.G. Smith, and K. Wayne, *Effects of train noise and vibration on human heart rate during sleep: an experimental study*. *BMJ Open*, 2013. doi:10.1136/bmjopen-2013-002655.
2. Smith, M.G., et al., *On the Influence of Freight Trains on Humans: A Laboratory Investigation of the Impact of Nocturnal Low Frequency Vibration and Noise on Sleep and Heart Rate*. *PLoS ONE*, 2013. **8**(2): p. e55829.
3. Alves Costa, P., R. Calçada, and A. Silva Cardoso, *Ballast mats for the reduction of railway traffic vibrations. Numerical study*. *Soil Dynamics and Earthquake Engineering*, 2012. **42**(0): p. 137-150.
4. Bongini, E., et al., *A parametric study of the impact of mitigation measures on ground borne vibration due to railway traffic*, in *EURODYN 2011*, G. De Roeck, et al., Editors. 2011: Leuven. p. 663-670.
5. Talbot, J. and H. Hunt, *On the Performance of Base-isolated Buildings and Isolation of Buildings from Rail-tunnel Vibration: a Review*, in *Collected Papers in Building Acoustics: Sound Transmission*, B. Gibbs, et al., Editors. 2009, Multi-science.
6. Talbot, J., *Base-isolated buildings: Towards performancebased design*. *Proceedings of the Institution of Civil Engineers: Structures and Buildings*, 2016. **169**(8): p. 574-582.
7. Hussein, M., M. Leamy, and M. Ruzzene, *Dynamics of Phononic Materials and Structures: Historical Origins, Recent Progress, and Future Outlook*. *Applied Mechanics Reviews*, 2014. **66**(4): p. 040802.

8. Lopes, P., et al., *Numerical Modeling of Vibrations Induced in Tunnels: A 2.5D FEM-PML Approach*, in *Traffic Induced Environmental Vibrations and Controls: Theory and Application*, H. Xia and R. Calçada, Editors. 2013, Nova. p. 133-166.
9. Achenbach, J.D., *Wave propagation in elastic solids*. Vol. 16. 1973, North-Holland: North-Holland Series in Applied Mathematics and Mechanics.
10. Lopes, P., et al., *Influence of soil stiffness on vibrations inside buildings due to railway traffic: numerical study*. *Computers & Geotechnics*, 2014. **61**: p. 277-291.
11. Amado-Mendes, P., et al., *2.5D MFS-FEM model for the prediction of vibrations due to underground railway traffic*. *Engineering Structures*, 2015. **104**: p. 141-154.
12. Coulier, P., et al., *Subgrade stiffening next to the track as a wave impeding barrier for railway induced vibrations*. *Soil Dynamics and Earthquake Engineering*, 2013. **48**: p. 119-131.
13. Barbosa, J., P. Alves Costa, and R. Calçada, *Abatement of railway induced vibrations: Numerical comparison of trench solutions*. *Engineering Analysis with Boundary Elements*, 2015. **55**(0): p. 122-139.